Journal of Materials and Environmental Science
ISSN : 2028-2508
e-ISSN : 2737-890X
CODEN : JMESCN

J. Mater. Environ. Sci., 2023, Volume 14, Issue 7, Page 762-784

http://www.jmaterenvironsci.com

Application of Response Surface Methodology to optimize the removal of caffeine and diclofenac from water using biochar produced from argan nutshells

Badr Bouhcain [1]*, Yassine Ez zoubi[1], Mohammed Hassani Zerrouk [1].**

[1] *Environmental Technologies, Biotechnology and Valorisation of Bio-Resources Team, TEBVB, FSTH, Abdelmalek Essaadi University, Tetouan, Morocco.*

** Corresponding Author: badr.bouhcain@etu.uae.ac.ma.*

*** Corresponding Author: m.hassani@uae.ac.ma*

Received *21 Mai 2023,*
Revised *04 July 2023,*
Accepted *06 July 2023*

Keywords:
- ✓ *Caffeine*
- ✓ *Diclofenac,*
- ✓ *Adsorption,*
- ✓ *Activated carbon,*
- ✓ *Response Surface methodology.*

Citation*: Bouhcain B., Ez zoubi M., Zerrouk M. H. (2023) Application of Response Surface Methodology to optimize the removal of caffeine and diclofenac from water using biochar produced from argan nut-shells, J. Mater. Environ. Sci., 14(7), 762-784*

Abstract: Caffeine and diclofenac, two representative anthropogenic indicators for wastewater pollution of surface waterways, have been adsorbed using agricultural activated carbon derived from argan nutshells (AN). Researchers have also focused on how changing factors including starting concentration, pH, temperature, adsorbent mass, and contact time affect the solid's adsorption behavior. To reduce costs and increase efficiency, models were developed using the data mining technique of response surface methodology (RSM), which considers a number of different operational factors. In this study, a variety of characterization techniques (FTIR, BET, and SEM) were utilized to analyze the adsorbent's properties with precision, allowing for a deeper insight into the material's structure and functionality. Adsorption was typically accomplished after a contact period of 90 minutes when 1 g of adsorbent material was added for both caffeine and diclofenac. As a further note, it has been shown that the adsorption of caffeine and diclofenac molecules to the sites of powdered biochar is significantly influenced by the initial concentration of pollutants, temperature, and pH variation. The highest removal percentages in the optimized step were obtained for RSM (Cf: Temperature 10 °C, adsorbent mass 0.8 g, contact time of 50 min, and caffeine concentrations of 100 mg/L), (Dcf: Temperature 20 °C, adsorbent mass 0.8 g, contact time of 50 min, and caffeine concentrations of 100 mg/L), and ANOVA analysis using the central composite design-response surface methodology indicated good agreement.

1. Introduction

In terms of abundance, water is one of the most essential substances in the cosmos (Karimi-Maleh et al., 2021b) (Karimi-Maleh et al., 2021a) (Karimi-Maleh et al., 2021c) Satisfying the ever-increasing need for drinkable water is a major pressing problem of the 21st century. As a result of climate change, overcrowding, industrialization, and environmental degradation, water demand is on the rise (Karimi-Maleh et al., 2020a) (Karimi-Maleh et al., 2020b) (Karimi-Maleh et al., 2020c). Massive quantities of drinkable water are discharged as wastewater, which, depending on the kind of activity, includes different impurities (GracePavithra et al., 2019).

Recent years have seen a significant rise in the number of research suggesting novel treatment methods for the removal of developing micropollutants, pesticides, fertilizers, medicines, plastics, and

personal care items from waterways. Many people consume new substances without knowing what impacts they may have on human health or what concentrations in water are safe for ecosystems, and standard wastewater treatment methods aren't very efficient at disposing of them (Verlicchi et al., 2013). Due to their toxicity, new forms of pollution present a significant threat to the ecosystem.

Among these contaminants, caffeine (Cf) is a non-regulated stimulant; after administration, most of it is metabolized, and only approximately 3% of the consumed amount is eliminated as Cf metabolites, theophylline, theobromine, and paraxanthine. Because of the high and human-related quantities of this chemical in water (Sauvé et al., 2012). Several scientists believe it to be a possible tracer of human pollution. In a study of 44 articles on the topic of the identification of emerging pollutants in wastewater, Cf was found to have the highest concentration among the compounds investigated, with an average value of 56.63 µg/L (Deblonde et al., 2011). Diclofenac (Dcf) is a nonsteroidal anti-inflammatory medicine and one of the most often identified pharmaceutical substances in wastewater treatment plant effluents (NSAID). Dcf has been shown in toxicology tests to have negative effects on human, plant, and animal life, even at very low concentrations in aqueous (Memmert et al., 2013).

It is feasible that species might acquire trace pollutants and pass them on to other creatures, posing a risk to human health. Biochar, a low-cost and effective adsorbent, has been utilized to deal with newly discovered toxins in water (Cheng et al., 2021) (Rout et al., 2021) (Delgado-Moreno et al., 2021). Adsorption processes are often not species-specific; therefore, they may be used to remove or significantly decrease a wide variety of pollutants (Gupta and Suhas, 2009).

Removal of drug substances from water may be accomplished through adsorption. There is a lot of interest right now in using carbon adsorbents made from renewable natural resources like coconut shells and husks, grape oil cakes, and other similar substances (Danish et al., 2021a; Bouhcain et al., 2021; Boujibar et al., 2018; Bernardo et al., 2016; Bouhcain et al., 2022; Torrellas et al., 2015; Danish et al., 2021b; Abo El Naga *et al.,* 2019; Avcu *et al*., 2021; Jodeh *et al.,* 2014; Kankou *et al*., 2021)). In this work, we investigated the adsorption of Dcf and Cf onto activated carbon made from carbonized Argan nutshells (AN).

Physical activation, chemical activation, or a mix of the two is used to create activated carbons from a wide variety of basic materials. Thus, we set out to investigate the feasibility of creating activated carbon from AN via the performance of relevant studies. During the process of extracting argan oil, AN (from Argania spinosa) is produced as agricultural waste. The Argania spinosa tree is native to Morocco and has spread to span an impressive 828,000 hectares of land. It produces 6,000 tons of argan oil per year and 27,000 tons of argan nut (AN) waste. As of right now, the AN waste is used as a fuel source for the locals (Zbair et al., 2018). However, like coconut shell, almond, or olive pomace, this biomass might be utilized as a renewable resource in the production of activated carbon.

In this study, we aim to determine optimal adsorption parameters for the effective elimination of emerging pollutants. Adsorption efficiency may be increased by enhancing the conditions in which it occurs. The adsorbent's surface area, the nature of the adsorbate, the initial concentration, the solution's pH, temperature, adsorbent dose, and contact time are all variables that might affect the efficiency of the removal process (Netzer and Hughes, 1984) (Bendjabeur et al., 2017) (Chuang et al., 2005).

The second part of our work involves modeling. Determining the ideal process conditions is, in fact, one of the fundamentals for the pre-design scale of any wastewater treatment system. Adsorption

is one of the water treatment procedures that involves a series of expensive and time-consuming studies to determine how input factors impact the process. The process design parameters have been optimized via the use of statistical and mathematical models to save time and money. In order to model and optimize an adsorption system, operational data must be collected in the absence of real testing. Single-variable, or classical, modeling approaches are laborious, expensive, and can't capture interactions between variables. To address these concerns, a variety of statistical methodologies were compiled into multivariate regression models to reveal the relationship between independent elements and provide more insight into the behaviors of the adsorption system. Response surface methodology (RSM) is a statistical tool for assessing the relationships between various inputs and the outcomes they produce (Nayak and Pal, 2020) (Igwegbe et al., 2019). By expressing the relationship between factors and responses using polynomial regression analysis, this mathematical method is able to find the optimal values for these variables.

2. Materials and methods

2.1. Materials

The AN activated carbon was used in this experiment was prepared from last work (Bouhcain et al., 2022), This sample was collected in Tafraout, Morocco (29°43′11.1″ N 8°58′51.7″ W), The activated carbon prepared with H_3PO_4 was named ACA. All of the compounds listed below were available commercially and were utilized without further preparation. Merck supplied phosphoric acid at a concentration of 85 %. Acros Organics provided Diclofenac sodium 98% (Dcf), while PanReac AppliChem supplied caffeine anhydrous 98.5% (Cf) (Belgium).

2.2. Methods

2.2.1. Characterization of the activated carbon

Surface functional groups have been identified using FTIR (Bruker Tensor II) spectroscopy. For FT-IR measurements, the material was mixed with KBr (sample: KBr = 2:200, w/w) to enhance the wavenumber range (400-4000 cm^{-1}). To obtain a background spectrum, a pure KBr pellet was applied.

In order to examine the AN morphology, a surface emission scanning electron microscope SEM (TESCON- Mira III XMU) was used in combination with an elemental analysis detector system (EDS) (Oxford Inst. INCA).

Nitrogen adsorption at 196 °C was used to investigate the textural quality of activated carbon using a Micrometrics ASAP 2420. (V_2.09). Using the Brunauer–Emmett–Teller (BET) equation, the specific surface areas (S_{BET}) of the isotherms were calculated. In addition, the total pore volume (V_{TP}) was estimated, which corresponds to the N_2 volume adsorbed at a relative pressure of 0.95 (P/P°). Using the t-plot approach, the volume of the micropores (VμP) and exterior surface area (S_{EXT}) were calculated. Using the difference between V_{TP} and VμP, the exterior volume (V_{EXT}) was determined. Utilizing the $4V_{TP}/S_{BET}$ ratio, the average pore diameter (D_{AP}) was calculated.

2.2.2. Adsorption of emerging contaminants

For adsorption to occur, the adsorbate must remain on the surface of the adsorbent without penetrating into the adsorbent's atomic structure. Batch adsorption tests were performed using IKA magnetic stirrers (RO-15) fitted with a Digiterm 100 microprocessor-controlled digital immersion thermostat and a thermostatic circulating bath. Also, a magnetic stir bar and a weight circle were

included to keep the solution from rising to the surface. Adsorbate solutions (C_0 = 100 mg/L) were added to a 50 mL-flask containing 1 g of activated carbon, and the time it took for the concentration of the adsorbate to reach equilibrium was measured. The experiments were undertaken at a steady temperature (10 °C) and a controlled shaking rate (200 rpm) until equilibrium was established. Qe (mg/g) is the amount of material adsorbed at equilibrium time and is a measure of adsorption capacity.

$$Qe = \frac{(Ce-Co)*V}{W} \quad \textbf{Eqn. 1}$$

$$Qt = \frac{(Ce-Ct)*V}{W} \quad \textbf{Eqn. 2}$$

where Co, Ct, and Ce (mg/L) represent the initial, time t, and equilibrium absorbate concentrations; W is the weight of adsorbent (g); and V is the volume of solution (L).

Adsorbent was removed from the solution using 0.45 µm syringe filters after equilibrium was attained, and the concentration of the adsorbate that was left behind was measured using a VWR UV-1600PC spectrophotometer. Maximum absorbance wavelengths (λmax) 290 nm for Cf and of 300 nm for Dcf were used throughout all tests.

2.2.3. Parameters influencing the mechanism of adsorption

Parameters which influence the mechanism of adsorption are:

2.2.3.1. pH of the solution

The adsorption efficiency is modified by the solution's pH. High adsorption of H^+ and OH ions dissociate functional groups on the adsorbent's active sites, altering reaction kinetics and equilibrium characteristics (Senthamarai et al., 2013) (Neeraj et al., 2016). Most contaminants have a negative charge, allowing biosorption with carbon and the solution's increased acidity very simple. Adsorbents are considered to be responsible for cation adsorption owing to the action of OH e ions at higher pH, whereas they preferentially adsorb anions at lower pH due to the presence of H^+ ions (Saravanan et al., 2020) (Foo and Hameed, 2010). When the pH is low, the concentration of H^+ ions increase, and the sorbents' positively charged surfaces attract more H^+ ions. Due to the positive charge of the adsorbent surface in acidic conditions, the adsorbate molecules become fully absorbed by the adsorbent. As the pH of the process increases, the number of negatively charged sites increases while the number of positively charged sites decreases. An anionic molecule can't immediately adsorb onto a sorbent with a negative charge layer site, since these layers exert repulsive forces on one another (Senthil Kumar et al., 2010).

2.2.3.2. Contact time

Adsorption efficiency, for instance, rises as contact time increases. There is an initial, strong increase in the quantity of adsorbate adsorbed onto the adsorbent surface, and then the process levels out and stabilizes at a constant value (Foo and Hameed, 2010).

2.2.3.3. Dosage of adsorbents

Specifically, the influence of adsorbent dose is the most important aspect to examine, as it determines the degree of adsorption and the cost of adsorbent per unit of solutions to process (Yaashikaa et al., 2019). When adsorbent dosage increases while all other parameters remain constant, the adsorption efficiency initially increases, reaches its maximum, and then begins to decrease (Padmavathy et al., 2016).

2.2.3.4. Initial concentration of adsorbate

A concentration gradient (the driving force) for mass transfer between the solution and the adsorbent is established by the initial concentration of the adsorbate in the solution (Senthil Kumar et al., 2014a). In the presence of a low initial adsorbate concentration, the adsorption rate and uptake capacity are less dependent on changes in the solute concentration. This is because a larger fraction of the solute molecules is attached to the adsorbate surface at the outset (Tharaneedhar et al., 2017). The adsorption uptake capacity is concentration dependent. Therefore, increasing the concentration lowers the ratio and increases the number of available adsorption sites for the adsorbate (Foo and Hameed, 2010). As a consequence, the uptake capacity will decrease with increasing initial concentration, but only slightly (Padmavathy et al., 2016) (Senthil Kumar et al., 2014c) (Senthil kumar and Kirthika, 2009).

2.2.3.5. Temperature

Temperature is still another important factor, since adsorption is often an exothermic process; hence, increasing the temperature would decrease the adsorption intensity. In general, temperature is inversely related to adsorption capacity. As the temperature rises, the solubility of the solute increases correspondingly; hence, the solubility of the adsorbate in the solvent will be greater than that of the adsorbent, which inhibits adsorption (Saravanan et al., 2018). In summary, temperature may affect the reversibility of the adsorption equilibrium by affecting both the adsorption and desorption processes (Foo and Hameed, 2010).

2.2.3.6. Adsorbate's nature

There is a strong correlation between the solubility of the adsorbate and the adsorption rate and capacity. The affinity of the solute with the solvent is strong if the adsorbate can be dissolved entirely in the solvent (S. and P., 2018). Consequently, the amount and rate of adsorption of this adsorbate are reduced. Therefore, it is conceivable to infer that the degree of adsorption is inversely related to the solubility of the solute (Grassi et al., 2012).

2.2.3.7. Surface area of adsorbent

Although adsorption occurs on surfaces, its strength depends on the available surface area, or the total free surface area for adsorption. This high surface area per unit mass of adsorbent is a reflection of the material's exceptionally fine and porous structure. In other words, if the surface area of the adsorbent is larger, the adsorption will be more effective (Rathi and Kumar, 2021).

2.2.4. Design of experiments

Statistical methods fall into three broad classes when used for the study of chemical processes in which several parameters influence the same response of interest. The circumstances of a process may be predicted using some of these methods. One of the most often used approaches in statistics is the response surface methodology (RSM). With RSM, we may examine the connection between a large number of predictors and a single or many responses. The RSM centers on the concept of carrying out a series of design experiments in order to arrive at the best possible result. Through the adjustment of process parameters, the maximum yield of a target material may be calculated using this approach. The essential aspects and properties of RSM are orthogonality, rotatability, and homogeneity. This method

often relies on experimentally designed data fits between empirical models and experimental data. In this research, RSM was used to analyze the factors that affect the efficacy of Cf and Dcf removal. Both the Central Composite Design (CCD) and the Box-Behnken Design (BBD) are included in RSM (BBD). RSM modeling included the use of the central composite design (CCD), with the four critical parameters being the initial concentration, the temperature, the contact time, and the mass of adsorbent, to account for the whole of the removal process. Design Expert, a statistical program, was used to plan a total of 29 trials. An analysis of variance (ANOVA) was performed to check the feasibility and significance of the projected model by assessing the goodness of fit, the regression coefficient (R^2), and the value of the Fisher variation ratio (F-value). After the model has been verified, it is shown as a three-dimensional graph that produces a surface response that may be used to determine the optimum operating parameters.

3. Results and discussions

3.1. Characterization of activated carbon

3.1.1. Fourier transformer infrared-spectroscopy (FTIR)

Figure 1 depicts the FTIR spectrum of argan nut shell, which exhibits an IR band at around 3416 cm^{-1} associated with O-H vibrations in hydroxyl groups. The band situated between about 2923 and 2852 cm^{-1} corresponds to the C-H vibrations of methyl and methylene compounds (El-Nabarawy et al., 1997) (Figueiredo et al., 1999). Furthermore, the band at 2349 cm^{-1} may be attributed to the carbon dioxide O=C=O stretching vibrations. The C-H bonds of aromatic compounds correspond to bending between 1958 and 1691 cm^{-1}. The peak centered at 1619 cm^{-1} corresponds to the aromatic C=C ring stretch (Bouchelta et al., 2008). In addition, the band between 1584 and 1329 cm^{-1} supports the existence of aromatic C-H compounds.

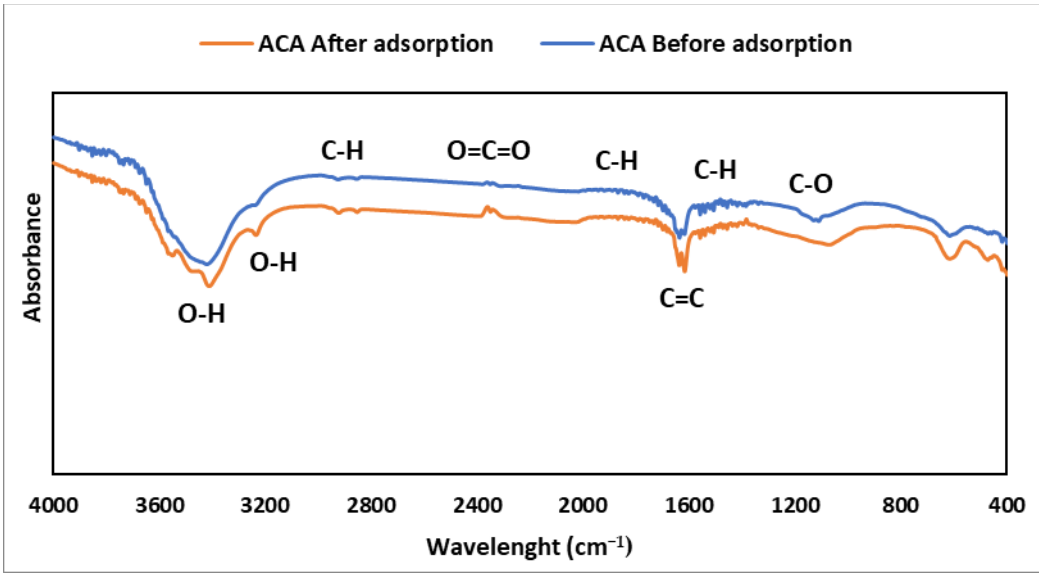

Figure 1. FT-IR spectrum of ACA before and after adsorption.

The strong peak recorded at 1105 cm^{-1} might also be attributable to C-O stretching vibrations. The 571 cm^{-1} IR band is responsible for the in-plane ring deformation (Ji et al., 2007). Adsorption has little effect on the FTIR spectra of ACA; the bands are comparable to those seen before adsorption, but the intensity of the bands is lower after adsorption. As a result, the other peaks vanished. This result suggested that the chemical activation method had successfully eliminated the majority of surface

functional groups. The FTIR findings are in agreement with the surface chemistries of other agricultural by-products such as raw cashew nut shell and pecan nutshell (Vaghetti et al., 2009) (Tangjuank et al., 2009).

3.1.2. Scanning-electron-microscopy-(SEM)

The scanning electron microscopy graphs (**Figure 2**) reveal that the ACA's surface was reasonably smooth and impermeable, except for the occasional crack. However, the chemical activation of activated carbons causes significant changes in the surface porosity, as seen in the morphology of the activated carbons. In addition, it seems that the roughness of the surface is augmented by the activating agent H_3PO_4. Porosity's growth is consistent with findings from the study of textures (**Table 1**).

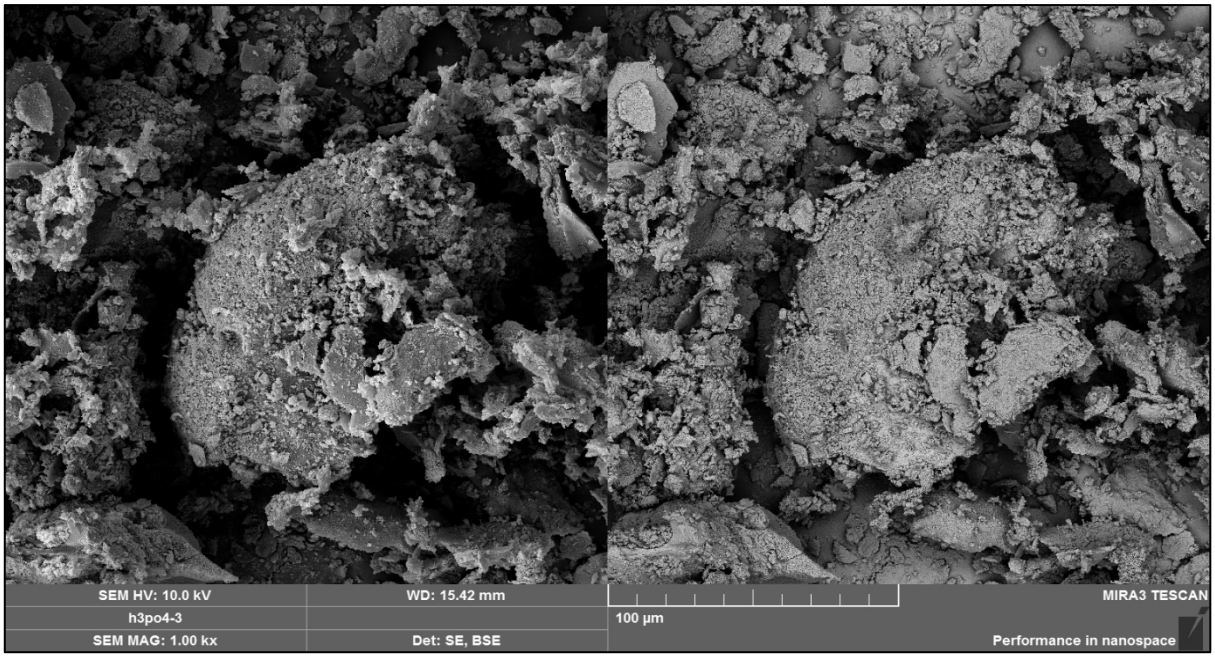

Figure 2. SEM image of ACA.

3.1.3. Specific Surface area analysis (BET)

At 77K, nitrogen physisorption was used to determine the ACA's textural properties. According to IUPAC classification (Thommes et al., 2015), it was obvious that ACA displayed the type II physisorption isotherm (**Figure 3**), which is typical of microporous materials. According to the data, phosphoric acid exhibited the greatest specific surface area, pore volume, and pore size dispersion (**Table 1**). These characteristics suggest that the generated activated carbon may be used as an effective adsorbent.

3.2. Caffeine and Diclofenac adsorption study

3.2.1. Effect of pH of the solution

Figure 4 illustrates the influence of pH on ACA adsorption at five different pH levels: 3, 5, 7, 9 and 11 for Cf (**Figure 4.B**) and five different pH levels: 4,6,7,8 and 10 for Dcf (**Figure 4.A**); utilizing 1 g of ACA with 100 mg/L of Cf and Dcf. 90 minutes were spent shaking the samples at 200 rpm at room temperature. The concentration of Cf or Dcf was then determined by the calibration curve using a VWR UV-1600PC spectrophotometer. Each study was conducted in duplicate.

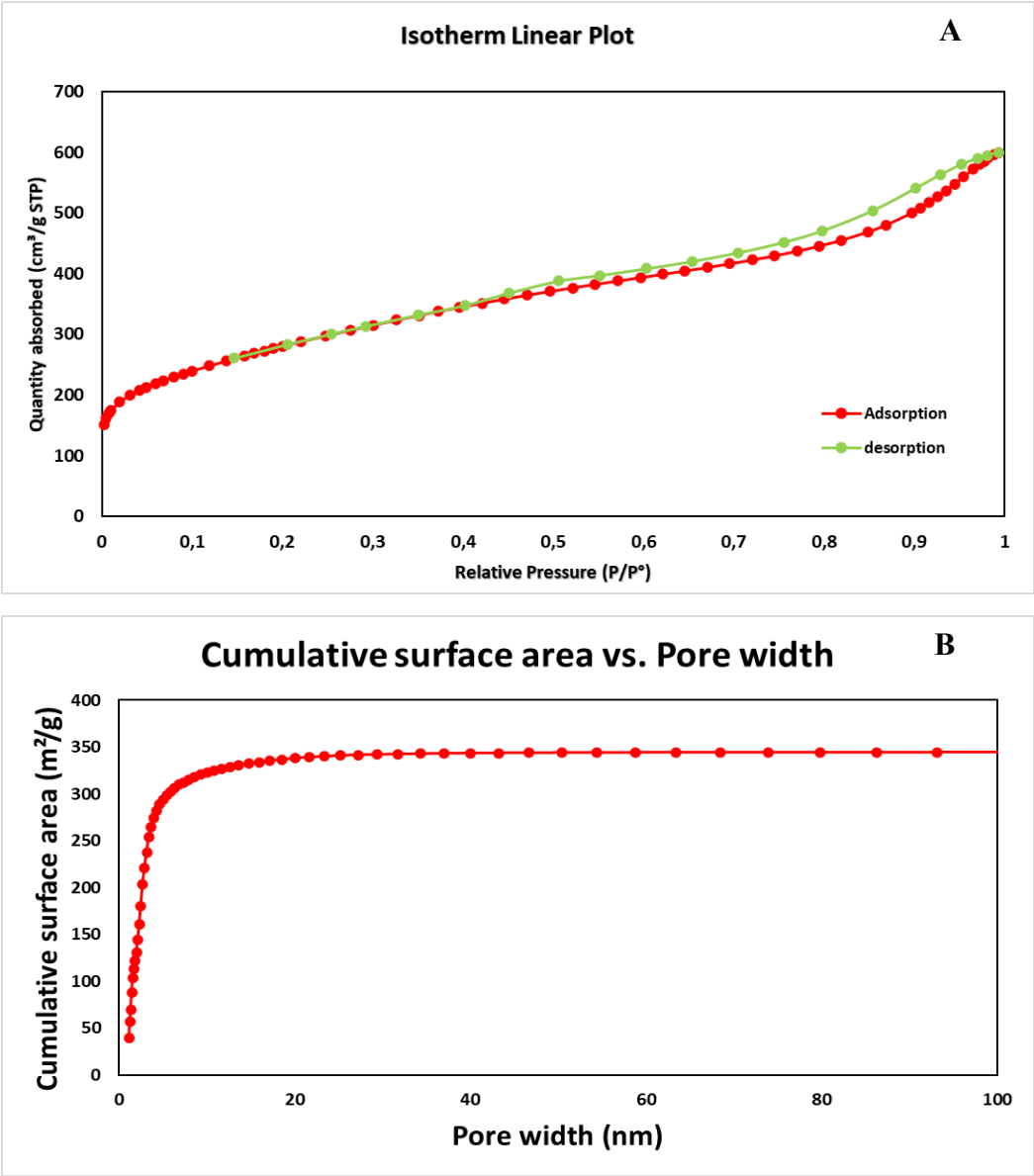

Figure 3. Nitrogen physisorption isotherm and pore size distributions of ACA.

Table 1. Textural properties of ACA.

Adsorbent	BET surface area (m^2/g)	Total pore volume (cm^3/g)	Average pore diameter (nm)
ACA	1007.76	0.85	3.38

Cf and Dcf adsorption is very dependent on the solution pH (Anastopoulos et al., 2020) (Beltrame et al., 2018) (Portinho et al., 2017); and numerous adsorption processes, such as hydrogen bonding, -interaction, etc., have been characterized. It has been shown that the ionization of pollutants and the surface charge of certain adsorbents are affected by the pH of the aqueous medium. **Figure 4.A** displays the results of an investigation into the efficiency of the Dcf adsorption process at pH values between 4 and 10. Diclofenac removal is inhibited by pH levels above 6, where the maximal adsorption capacity of the Dcf is maximized (89%). An adsorbent pHpzc of 6.5 was determined (**Figure 4.C**) Due to the repulsive electrostatic interaction between the anionic species of the target pollutant and the negative charge on the adsorbent surface, the adsorption capacity is reduced in an alkaline solution (pH

approximately 10). These results correspond to the findings of Li et al (Li et al., 2018), who investigated the feasibility of using activated carbon to precipitate sodium diclofenac from water.

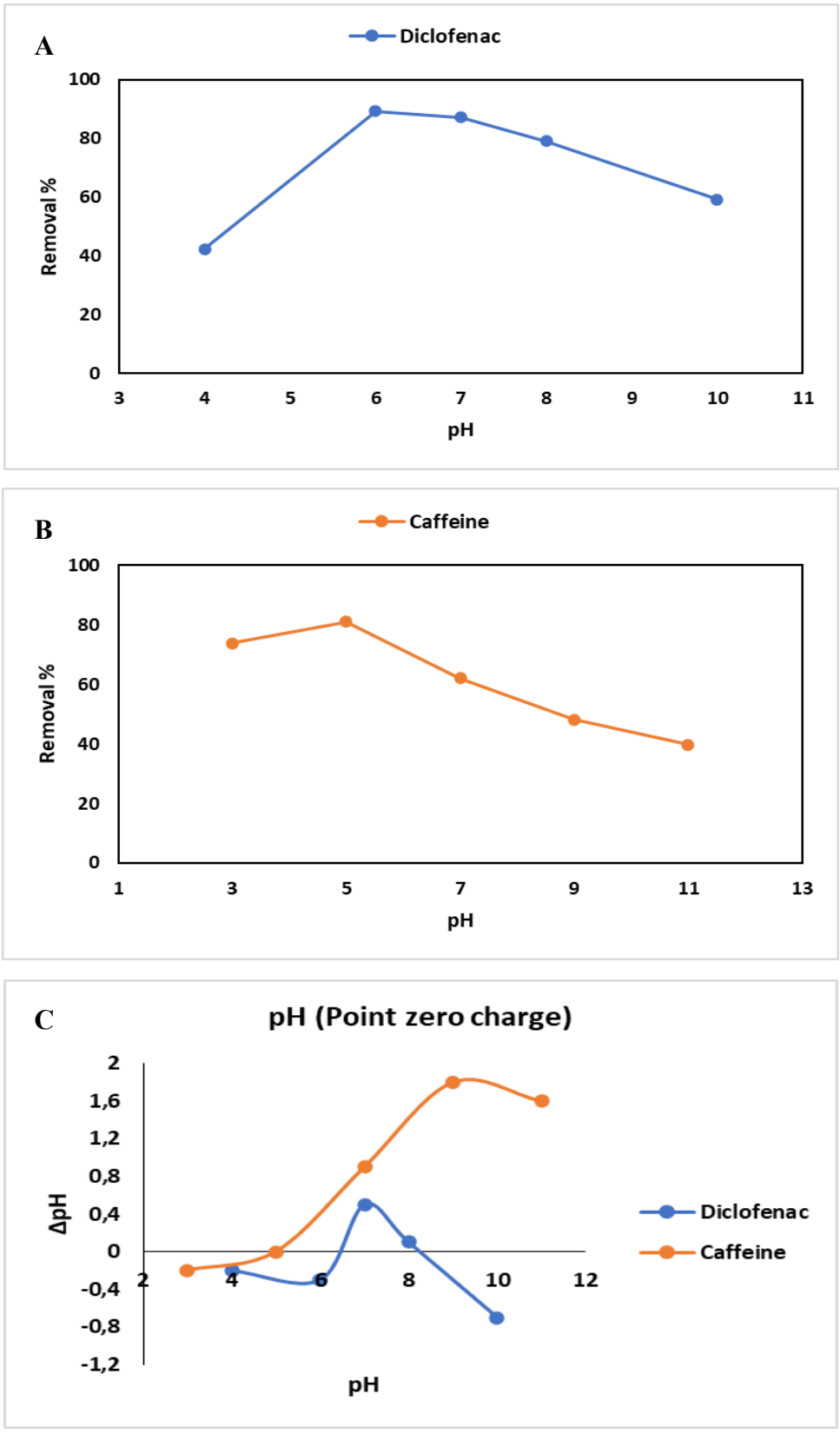

Figure 4. Effect of pH over adsorption process.

Cf adsorption is shown to be affected by an initial pH range of 3-11 (**Figure 4.B**). Figure reveals that between 5 and 7 pH, the adsorption is highest (81%). The adsorbent was measured to have a pHpzc of 5, which is neutral (**Figure 4.C**). Therefore, the ACA surface will be mostly negatively charged at pH > 5, and positively charged at pH 5. Electrostatic interaction between ACA and the neural form of caffeine explains why the maximum adsorption capacity of caffeine on ACA was found at pH values between 5 and 7, and why this capacity was dramatically decreased at pH values between 7 and 11. Caffeine's microporous structure is less permeable at high pH because the molecule is mostly negatively charged and more permeable at low pH because it is predominantly positively charged.

3.2.2. Effect of mass of adsorbent

Figure 5 demonstrates that both Cf and Dcf adsorption capacities improve with increasing adsorbent dose. This has been shown by several studies (Portinho et al., 2017) (Ahmad et al., 2013) (Gil et al., 2018) (Luján-Facundo et al., 2019) (Melo et al., 2020) (Nam et al., 2014) (Westerhoff et al., 2005). When the quantity of adsorbent rises, the availability of active sites increases, hence enhancing the Cf and Dcf adsorption performance (Ahmad et al., 2013) (Al-Khateeb et al., 2014). However, the expense of the adsorption process might rise with the use of large amounts of adsorbent. This means that finding the right amount of activated carbon to use is crucial for cost-effectiveness (Portinho et al., 2017). Moreover, Nam et al. (Nam et al., 2014) observed caffeine removal efficiencies of 80–90% at activated carbon concentrations larger than 5 mg/L. Increasing the amount of activated carbon to 20 mg resulted in a negligible (5%) improvement in the removal efficiency for Cf.

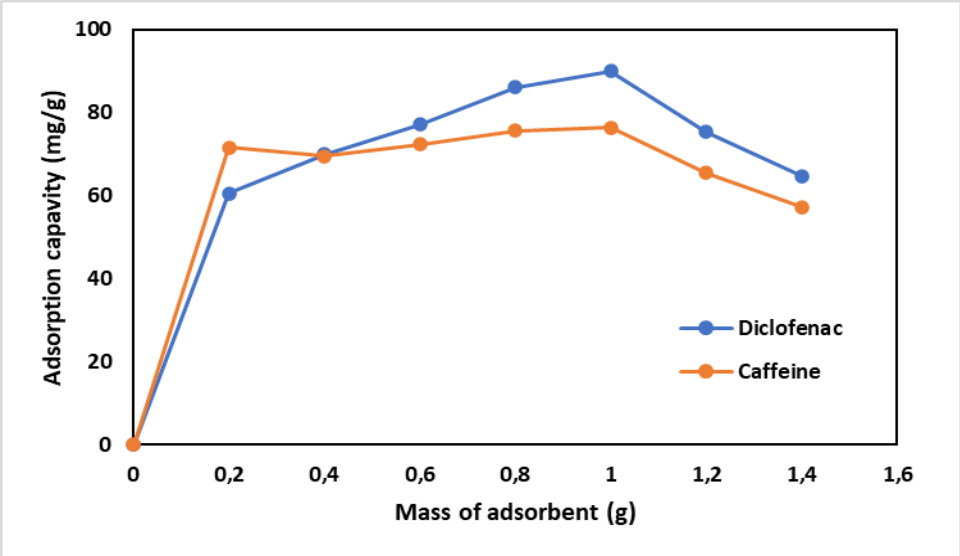

Figure 5.-Effect of mass of adsorbent over adsorption process.

3.2.3. Effect of initial concentration of adsorbate

For the first adsorbate concentration tests, 1 g of ACA was mixed for 90 minutes at 10 °C with solutions ranging from 10 to 120 mg/L. **Figure 6** depicts the outcomes achieved. When the initial concentration is low, the ratio of the number of solute molecules to the Dcf and Cf surfaces is low. The initial concentration of the solute has minimal effect on the sorption rate and absorption capacity. Eventually, the sorption capacity becomes independent of the original solute concentration (Thekkudan *et al.,* 2017). In addition, the ratio rises at high concentrations, showing that there are fewer vacant adsorption sites for adsorbate, and the sorption capacity is dependent on the initial concentration (Foo

and Hameed, 2010). As a consequence, the absorption capacity decreases as initial concentrations increase (Padmavathy *et al.,* 2016) (Senthil Kumar *et al.*, 2014b) (Senthil kumar and Kirthika,, 2009).

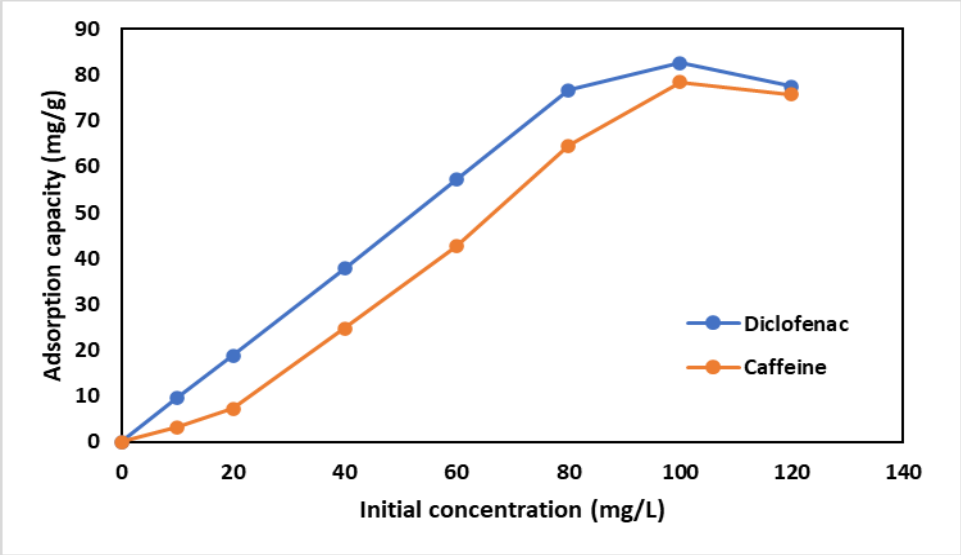

Figure 6. Effect of initial concentration over adsorption process.

3.2.4. Effect of contact time

Adsorption of Cf and Dcf onto the ACA was demonstrated to grow gradually over time and achieve equilibrium after 90 min (**Figure 7**). The mass transfer resistance of the organic chemical between the aqueous and solid phases is likely overcome by the concentration gradient. As a result, the capacity for adsorption increases, up to a point when it becomes saturated. Adsorption occurred in two phases: a short period of intense absorption occurring within minutes (up to 30 min), followed by a prolonged period of significantly slower uptake. Adsorption was more rapid in the first phase because of the abundance of active sites on the adsorbent and the contact between the adsorbent's surface and the organic molecule. Repulsive forces between organic molecules already adsorbed on the solid surface and those in the bulk phase may account for the eventual decreased adsorption.

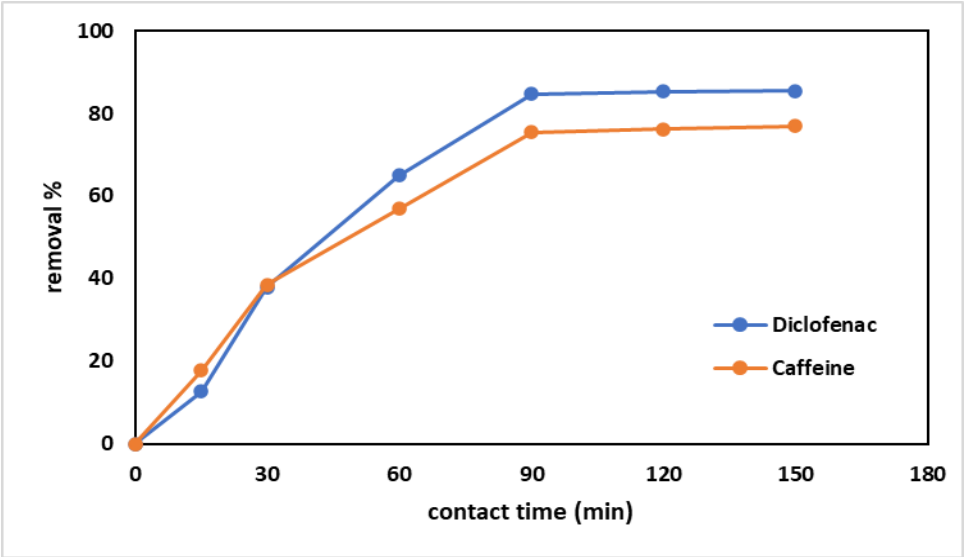

Figure 7. Effect of contact time over adsorption process.

2.5. Effect of temperature

The adsorption of Dcf and Cf by ACA may be affected by a number of factors, including temperature, that are associated with the adsorbent and the gas being adsorbed. In this case, we conducted studies at five distinct temperatures (at 10, 20, 30, 40, and 50 degrees Celsius) to observe how these variables affected the effectiveness of waste removal. **Figure 8** demonstrates that, as expected, ACA's adsorption capability declined with rising temperature. Adsorption of Cf reduced from 84% to 40%, while Dcf elimination efficiency dropped from 90% to 48%. Adsorption of these pollutants may have decreased because of desorption brought on by an increase in thermal energy. The balance between adsorption and desorption shifts as a result. Early on in the process of removing the substance, adsorption occurred quickly. After 90 minutes, there was no discernible change in adsorption capacity up to 150 minutes, when equilibrium was reached. The high BET surface area of ACA suggests that it is responsible for the rapid initial adsorption rate. The rapid establishment of equilibrium is beneficial for the application of ACA in the removal of pollutants at room temperature.

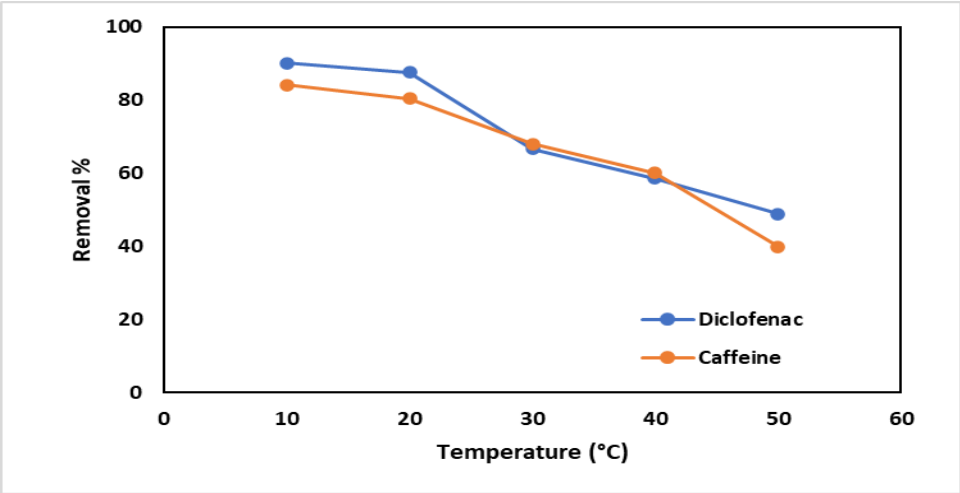

Figure 8. Effect of temperature over adsorption process.

3.3. RSM modelling and optimization

Table 2 illustrates the final experimental design matrix and response outcomes under various experimental conditions. **Table 2.A** shows that adsorption efficiencies for Cf range from 31.04% to 98.79%, whereas **Table 2.B** shows that efficiencies for Dcf range from 27.55% to 98.90%. In **Eqn. 3**, we offer the final studied (and coded) RSM model for Cf and Dcf adsorption, which allows us to assess and anticipate the ideal circumstances for higher efficiency. The coefficient's positive sign in this empirical equation denotes the component that positively affects adsorption, whereas the negative sign denotes the term that negatively affects adsorption. Statistical research reveals that the removal efficiency of Dcf and Cf is favorably influenced by interactions involving temperature and contact time, temperature and mass of adsorbent, initial concentration, and contact time and initial concentration, mass of adsorbent, and initial concentration. On the other hand, a negative effect is shown in the interactions between initial concentration and contact time, temperature, and contact time, as well as between contact time and adsorbent mass:

$$\boldsymbol{Adsorption} = +47.11 - 2.82\,A\; - 0.06\,B\; + 0.23\,C\; + 114.48\,D\; + 0.004\,AB - 0.016\,AC + 0.45\,AD\; + 0.001\,BC\; - 0.01\,BD\; + 0.27\,CD\; + 0.07A^2 - 0.0004\,B^2 - 0.001C^2 - 60.7\,D^2 \qquad \textbf{Eqn. 3}$$

Table 2.A. The central composite design's experimental Cf runs and responses.

Cf	Run	Temperature (°C)	Time (min)	initial concentration (mg/L)	Dose (g)	Absorbance	Ce (mg/L)	Ci-Ce (mg/L)	Removal efficiency %
29	1	20	50	75	0.8	0.086	10.42	64.58	86.10
18	2	30	50	50	0.8	0.022	2.67	47.33	94.67
15	3	20	10	100	0.8	0.176	21.33	78.67	78.67
26	4	20	50	75	0.8	0.087	10.54	64.46	85.94
1	5	10	10	75	0.8	0.046	5.58	69.42	92.57
12	6	30	50	75	1.4	0.028	3.39	71.61	95.48
8	7	20	50	100	1.4	0.069	8.36	91.64	91.64
22	8	20	90	75	0.2	0.386	46.78	28.22	37.62
4	9	30	90	75	0.8	0.027	3.27	71.73	95.64
7	10	20	50	50	1.4	0.06	7.27	42.73	85.46
23	11	20	10	75	1.4	0.062	7.51	67.49	89.98
10	12	30	50	75	0.2	0.401	48.60	26.40	35.20
24	13	20	90	75	1.4	0.062	7.51	67.49	89.98
25	14	20	50	75	0.8	0.091	11.03	63.97	85.29
2	15	30	10	75	0.8	0.106	12.85	62.15	82.87
16	16	20	90	100	0.8	0.123	14.91	85.09	85.09
9	17	10	50	75	0.2	0.345	41.81	33.19	44.25
5	18	20	50	50	0.2	0.243	29.45	20.55	41.10
6	19	20	50	100	0.2	0.569	68.96	31.04	31.04
17	20	10	50	50	0.8	0.024	2.91	47.09	94.18
27	21	20	50	75	0.8	0.091	11.03	63.97	85.29
20	22	30	50	100	0.8	0.191	23.15	76.85	76.85
19	23	10	50	100	0.8	0.01	1.21	98.79	98.79
21	24	20	10	75	0.2	0.397	48.12	26.88	35.84
14	25	20	90	50	0.8	0.072	8.73	41.27	82.55
11	26	10	50	75	1.4	0.012	1.45	73.55	98.06
3	27	10	90	75	0.8	0.012	1.45	73.55	98.06
28	28	20	50	75	0.8	0.113	13.70	61.30	81.74
13	29	20	10	50	0.8	0.079	9.57	40.43	80.85

3.3.1. Analysis of variance (ANOVA)

Table 3 is a summary of the analysis of variance for ACA's effectiveness in removing Cf and Dcf. The generated quadratic model was shown to be statistically significant (P 0.05) by the findings. **Table 3.A** lists the most important model terms for Cf, and **Table 3.B** lists the most important model terms for Dcf. In addition, **Table 3** demonstrates that the quadratic model's lack of fit F-values is statistically significant (p 0.05). When all other variables are maintained constant, the estimated coefficient is the predicted shift in reaction per unit shift in factor value. In an orthogonal design, the intercept represents the mean response over all iterations. Coefficients are scale factors that modify that mean value. VIFs of 1 show that the factors are orthogonal; VIFs larger than 1 imply multi-collinearity, with higher values indicating stronger correlations between components. VIFs below 10 are generally considered acceptable.

Table 2.B. The central composite design's experimental Dcf runs and responses.

Dcf	Run	Temperature (°C)	Time (min)	initial concentration (mg/L)	Dose (g)	Absorbance	Ce (mg/L)	Ci-Ce (mg/L)	Removal efficiency %
29	1	20	50	75	0.8	0.132	10.14	64.86	86.48
18	2	30	50	50	0.8	0.163	13.31	36.69	73.38
15	3	20	10	100	0.8	0.335	30.91	69.09	69.09
26	4	20	50	75	0.8	0.119	8.81	66.19	88.26
1	5	10	10	75	0.8	0.198	16.89	58.11	77.48
12	6	30	50	75	1.4	0.107	7.58	67.42	89.89
8	7	20	50	100	1.4	0.045	1.24	98.76	98.76
22	8	20	90	75	0.2	0.488	46.56	28.44	37.91
4	9	30	90	75	0.8	0.195	16.58	58.42	77.89
7	10	20	50	50	1.4	0.052	1.95	48.05	96.09
23	11	20	10	75	1.4	0.041	0.83	74.17	98.90
10	12	30	50	75	0.2	0.551	53.01	21.99	29.32
24	13	20	90	75	1.4	0.049	1.65	73.35	97.81
25	14	20	50	75	0.8	0.096	6.45	68.55	91.39
2	15	30	10	75	0.8	0.287	26.00	49.00	65.34
16	16	20	90	100	0.8	0.211	18.22	81.78	81.78
9	17	10	50	75	0.2	0.468	44.52	30.48	40.64
5	18	20	50	50	0.2	0.382	35.72	14.28	28.56
6	19	20	50	100	0.2	0.741	72.45	27.55	27.55
17	20	10	50	50	0.8	0.049	1.65	48.35	96.71
27	21	20	50	75	0.8	0.139	10.85	64.15	85.53
20	22	30	50	100	0.8	0.392	36.74	63.26	63.26
19	23	10	50	100	0.8	0.056	2.36	97.64	97.64
21	24	20	10	75	0.2	0.509	48.71	26.29	35.05
14	25	20	90	50	0.8	0.048	1.54	48.46	96.91
11	26	10	50	75	1.4	0.047	1.44	73.56	98.08
3	27	10	90	75	0.8	0.045	1.24	73.76	98.35
28	28	20	50	75	0.8	0.115	8.40	66.60	88.80
13	29	20	10	50	0.8	0.116	8.50	41.50	83.00

Table 3.A. Analysis of variance for the central composite design (Cf).

Source	Sum of Squares	df	Mean Square	F-value	p-value	
Model	13624.86	14	973.20	65.95	< 0.0001	Significant
A-Temperature	180.19	1	180.19	12.21	0.0036	Significant
B-Time	66.08	1	66.08	4.48	0.0527	Non-Significant
C-Initial concentration	42.35	1	42.35	2.87	0.1124	Non-Significant
D-Dose	9078.74	1	9078.74	615.25	< 0.0001	Significant
AB	13.22	1	13.22	0.8959	0.3599	Non-Significant
AC	68.93	1	68.93	4.67	0.0485	Significant
AD	30.19	1	30.19	2.05	0.1746	Non-Significant
BC	5.59	1	5.59	0.3785	0.5483	Non-Significant
BD	0.7900	1	0.7900	0.0535	0.8204	Non-Significant
CD	65.94	1	65.94	4.47	0.0529	Non-Significant
A^2	387.88	1	387.88	26.29	0.0002	Significant
B^2	2.91	1	2.91	0.1975	0.6635	Non-Significant
C^2	7.14	1	7.14	0.4838	0.4981	Non-Significant
D^2	3101.09	1	3101.09	210.16	< 0.0001	Significant
Residual	206.59	14	14.76			
Lack of Fit	193.76	10	19.38	6.04	0.0489	Significant
Pure Error	12.83	4	3.21			
Cor Total	13831.45	28				

Table 3.B. Analysis of variance for the central composite design (Dcf).

Source	Sum of Squares	df	Mean Square	F-value	p-value	
Model	17901.72	4	1278.69	28.30	< 0.0001	Significant
A-Temperature	1485.04	1	1485.04	32.86	< 0.0001	Significant
B-Time	417.78	1	417.78	9.25	0.0088	Significant
C-Initial concentration	174.71	1	174.71	3.87	0.0694	Non-Significant
D-Dose	13351.73	1	13351.73	295.48	< 0.0001	Significant
AB	51.30	1	51.30	1.14	0.3047	Non-Significant
AC	25.14	1	25.14	0.5563	0.4681	Non-Significant
AD	2.68	1	2.68	0.0593	0.8111	Non-Significant
BC	0.3769	1	0.3769	0.0083	0.9285	Non-Significant
BD	0.2280	1	0.2280	0.0050	0.9444	Non-Significant
CD	5.07	1	5.07	0.1121	0.7427	Non-Significant
A^2	38.68	1	38.68	0.8561	0.3705	Non-Significant
B^2	42.56	1	42.56	0.9418	0.3483	Non-Significant
C^2	36.60	1	36.60	0.8099	0.3834	Non-Significant
D^2	2367.11	1	2367.11	52.39	< 0.0001	Significant
Residual	632.61	14	45.19			
Lack of Fit	612.01	10	61.20	11.88	0.0146	Significant
Pure Error	20.60	4	5.15			
Cor Total	18534.33	28				

Table 4 shows a satisfactory fit between the experimental and projected data, reflecting the significance of the variance around the mean described by the model. Meanwhile, the normal probability curves of the residuals (% normal probability compared to the residuals examined internally) show (**Figure 9**) that the estimated values are extremely close to the experimental values.

3.3.2. Response surface morphology (RSM)

As shown in **Figure 10.A** and **10.B**, the three-dimensional response plots and their related contour lines for Cf and Dcf removal efficiency illustrate the effect of the selected factors and their interactions on the response. Two of the four parameters were changeable, while the other two were fixed. **Figure 10.A** illustrates the impact of initial concentration on Cf adsorption. As observed, the adsorption effectiveness improved as the initial Cf concentration. When the adsorbent mass and temperature are held constant, the adsorption falls as the Cf concentration increases. The impact of solution temperature on adsorption is seen in **Figure 10.A**. It was clearly shown that the adsorption of Cf decreased as the temperature decreased. Even though the mass of the adsorbent increased at a fixed initial concentration, its adsorption effectiveness decreased owing to the saturation of its active sites. While the greater initial concentration at a lower mass of ACA increases its adsorption, the converse is not true. **Figure 10.A** depicts the influence of adsorbent mass on adsorption efficiency and its relationship with contact time. When the initial concentration and temperature are held constant, it is shown that more than 98% of Cf is adsorbed in the first 50 minutes with an adsorbent mass that ranges from about 0.8 g. A response surface approach was used to determine the appropriate proportions of the various independent factors for Cf elimination. Maximum adsorption was attained at an initial concentration of 100 mg/L, adsorbent mass of 0.8 g, temperature of 10 °C, and contact time of 50 minutes. After optimizing the independent variables, the final adsorption test was conducted at the ideal level to validate the model's validity. The effect of initial concentration on Dcf adsorption is seen in **Figure 10.B.** As can be observed, a higher initial concentration of Dcf improves adsorption efficiency.

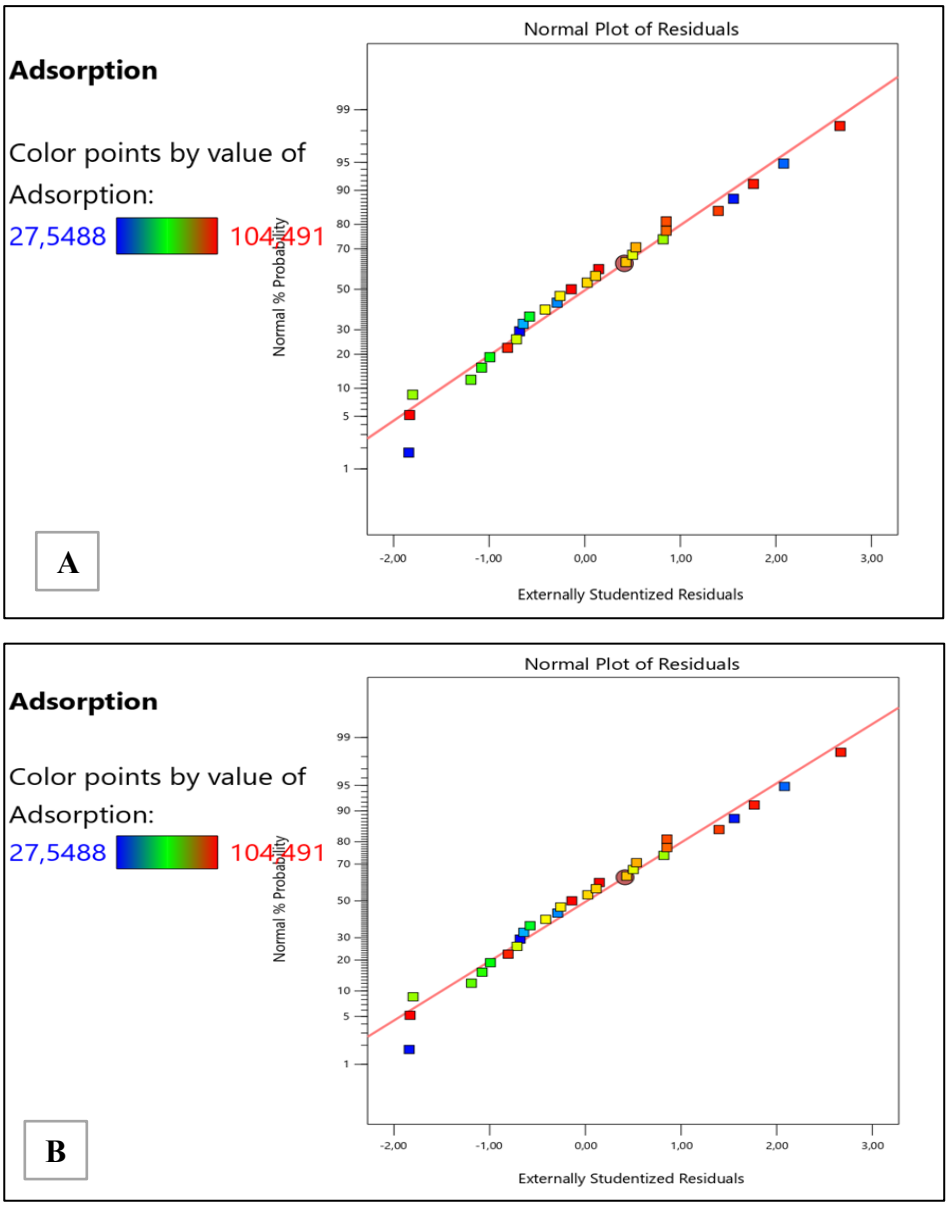

Figure 9. Study of the adsorption of caffeine (A) and diclofenac (B) onto ACA, as measured by their respective normal % probability residuals and studentized residuals.

Table 4.A. Fit summary of the polynomial deviation around the mean explained by the model (Cf).

Source	Sequential p-value	Lack of Fit p-value	Adjusted R^2	Predicted R^2
Linear	< 0.0001	0.0004	0.6235	0.5024
2FI	0.9909	0.0002	0.5187	0.0099
Quadratic	**< 0.0001**	**0.0489**	**0.9701**	**0.9179**
Cubic	0.0749	0.1202	0.9875	0.7469

Table 4.B. Fit summary of the polynomial deviation around the mean explained by the model (Dcf).

Source	Sequential p-value	Lack of Fit p-value	Adjusted R^2	Predicted R^2
Linear	< 0.0001	0.0023	0.8045	0.7540
2FI	0.9972	0.0013	0.7465	0.5343
Quadratic	**0.0001**	**0.0146**	**0.9317**	**0.8081**
Cubic	0.0420	0.0516	0.9772	0.4536

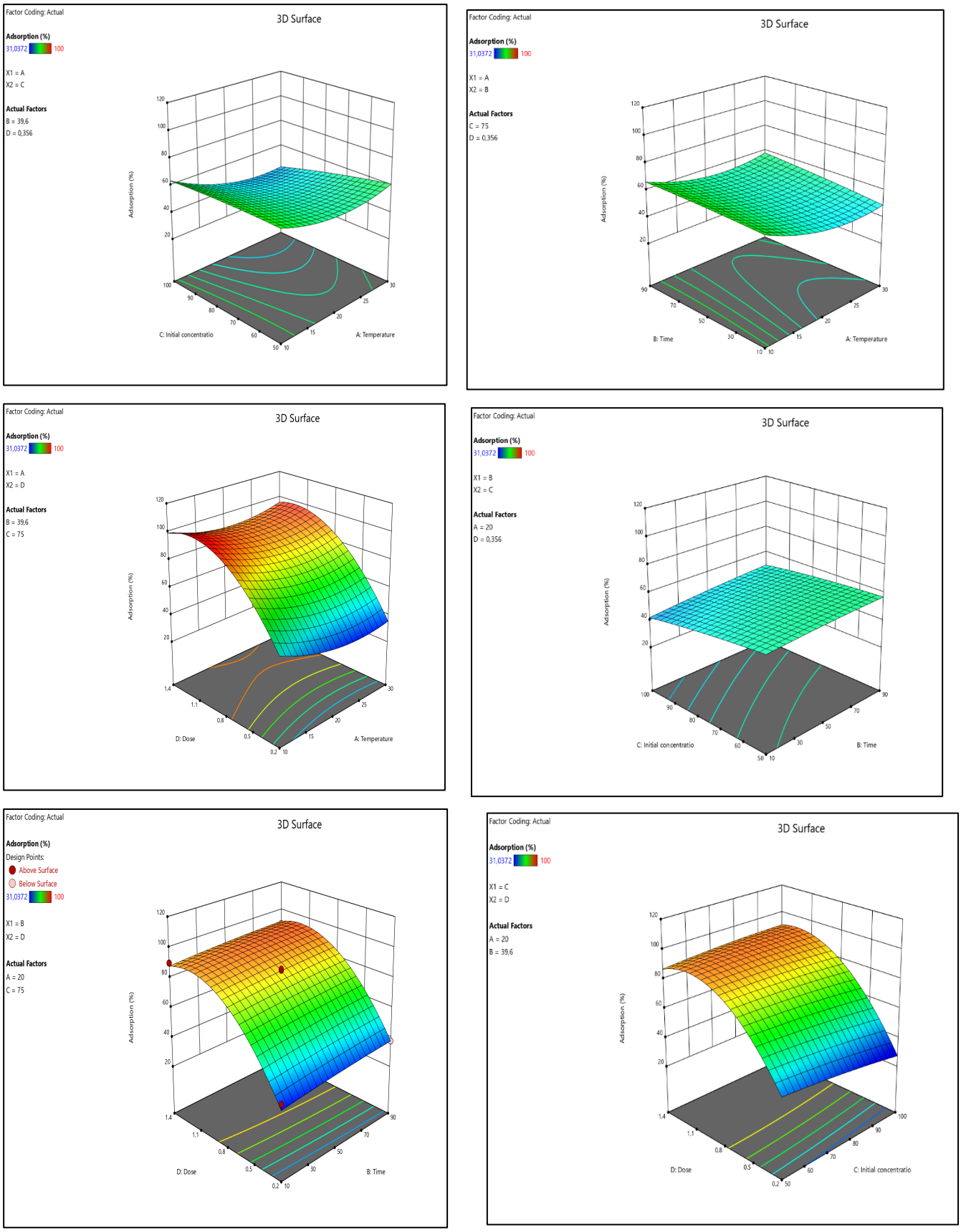

Figure 10.A. Cf removal efficiency surface and contour plots.

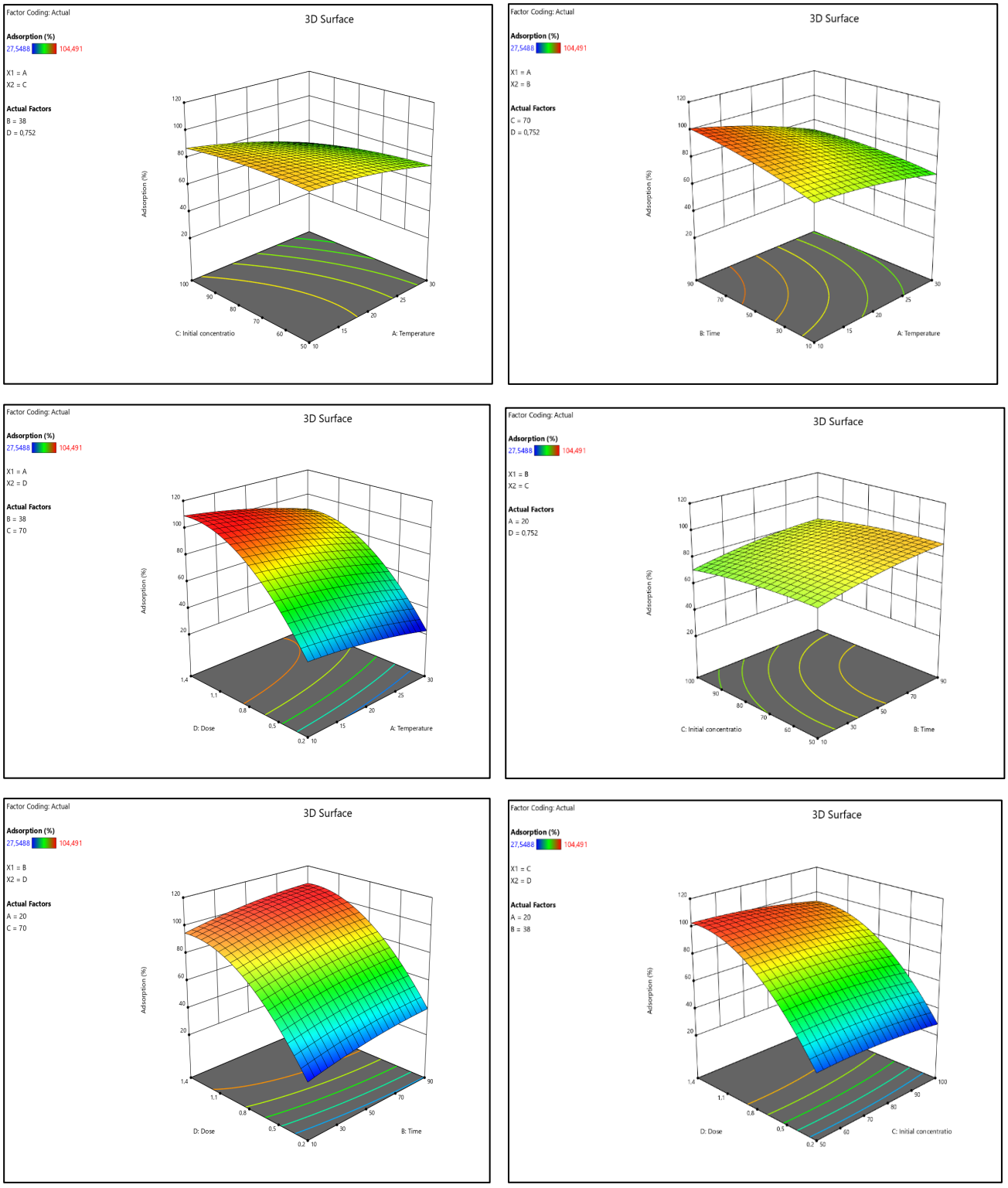

Figure 10.B. Dcf removal efficiency surface and contour plots.

Given a certain amount of adsorbent mass and a fixed temperature, a higher Dcf concentration results in lower adsorption. **Figure 10.B** shows how the solution temperature affects adsorption. Adsorption of Cf was seen to decrease when the temperature was lowered, supporting the hypothesis that Cf is temperature sensitive. Since the active sites were saturated as the adsorbent mass increased for a given initial concentration, the adsorption efficiency decreased. While ACA's adsorption is

enhanced by a smaller mass at a greater initial concentration, the converse is not true. **Figure 10.B** depicts the interplay between adsorbent mass and contact time with regards to adsorption effectiveness. More than 98% of Cf is adsorbed in the first 10 min with a mass of adsorbent that changes about 0.8 g when the initial concentration and temperature are held constant. With the help of the response surface approach, we were able to determine the ideal ranges for all of the variables in the process of eliminating Dcf. At an initial concentration of 75 mg/L, the adsorbent mass of 1.4 g, a temperature of 20 °C, and a contact time of 10 min, 98.90% adsorption was obtained. As a last step in ensuring the model's accuracy, the adsorption assay was conducted with all independent variables set to their best possible values.

3.3.3. Optimization

An initial Cf concentration of 100 mg/L, temperature of 10 °C, a contact time of 50 minutes, and an adsorbent mass of 0.8 g were found to be optimal for Cf adsorption. The experiments were run under ideal circumstances to ensure that the optimization held up. Response values under ideal circumstances were measured and compared to projected values. The experimental data was the observed value, and the anticipated value was determined by using Eq (3). A good agreement between the anticipated and observed values was found, with a 90.67% observed value and a 95.83% projected value. As a result, the efficacy of the model was verified. Initial Dcf concentration of 75 mg/L, temperature of 20 °C, contact time of 10 min, and adsorbent mass of 1.4 g were determined to be optimal for the adsorption of Dcf. In order to verify the optimization, experiments were conducted under optimal circumstances. The contrast between observed and expected response levels under ideal circumstances was investigated. The experiment's observed value was the measured data, and the anticipated value was determined using **Eqn. 3**. The actual value was 79.92% whereas the expected value was 92.14% indicating that the predicted and observed values were in excellent agreement. Consequently, the performance of the model was verified.

Conclusion

Finally, two emerging contaminants, caffeine and diclofenac, have been removed from aqueous solutions by adsorption using activated carbon from argan nutshells (ACA). Considering the large surface area available to the chemical compounds, it is not unexpected that the material has a similar sorption capacity for the two adsorbates. After 90 minutes of contact, equilibrium was often reached in the compound/carbon systems. This study explores its potential as a tool for purifying water systems by removing caffeine and diclofenac. ACA was characterized using BET, SEM, and FTIR to explain its structure and surface properties. RSM was used to determine the optimum values for the process variables involved in the elimination of caffeine and diclofenac by ACA (solution pH, initial concentration, adsorbent mass, temperature, and contact time). As part of the RSM strategy, the cubic regression model was developed. The RSM designed for describing the elimination of diclofenac and caffeine passed the ANOVA test, showing its suitability for the task. The findings showed that the model's predictions were in excellent agreement with the experimental data, with a high correlation value (R^2 = Cf (0.9701), Dcf (0.9317)). The high adsorption capacity and their cost-effective synthesis demonstrated the significant potential of ACA for use in practical settings.

Disclosure statement: *Conflict of Interest:* The authors declare that there are no conflicts of interest.
Compliance with Ethical Standards: This article does not contain any studies involving human or animal subjects.

References

Abo El Naga A.O., El Saied M., Shaban S.A., El Kady F.Y. (2019). Fast removal of diclofenac sodium from aqueous solution using sugar cane bagasse-derived activated carbon. *J. Mol. Liq.* 285, 9–19. https://doi.org/10.1016/j.molliq.2019.04.062

Ahmad L.O., Linh L.H.M., Akimoto M., Kaneki Y., Honda M., Suda M., Kunimoto K.-K., (2013). Persimmon Tannin Gel: Formation by Autoxidation and Caffeine Adsorption Properties. *Food Sci. Technol. Res.* 19, 697–703. https://doi.org/10.3136/fstr.19.697

Al-Khateeb L.A., Almotiry S., Salam M.A. (2014). Adsorption of pharmaceutical pollutants onto graphene nanoplatelets. *Chem. Eng. J.* 248, 191–199. https://doi.org/10.1016/j.cej.2014.03.023

Anastopoulos I., Katsouromalli A., Pashalidis I. (2020). Oxidized biochar obtained from pine needles as a novel adsorbent to remove caffeine from aqueous solutions. *J. Mol. Liq.* 304, 112661. https://doi.org/10.1016/j.molliq.2020.112661

Avcu T., Üner O., Geçgel Ü. (2021). Adsorptive removal of diclofenac sodium from aqueous solution onto sycamore ball activated carbon – isotherms, kinetics, and thermodynamic study. *Surf. Interfaces* 24, 101097. https://doi.org/10.1016/j.surfin.2021.101097

Beltrame K.K., Cazetta A.L., de Souza P.S.C., Spessato L., Silva T.L., Almeida V.C. (2018). Adsorption of caffeine on mesoporous activated carbon fibers prepared from pineapple plant leaves. Ecotoxicol. Environ. Saf. 147, 64–71. https://doi.org/10.1016/j.ecoenv.2017.08.034

Bendjabeur S., Zouaghi R., Kaabeche O.N.H., Sehili T. (2017). Parameters Affecting Adsorption and Photocatalytic Degradation Behavior of Gentian Violet under UV Irradiation with Several Kinds of TiO2 as a Photocatalyst. *Int. J. Chem. React. Eng.* 15. https://doi.org/10.1515/ijcre-2016-0206

Bernardo M., Rodrigues S., Lapa N., Matos I., Lemos F., Batista M.K.S., Carvalho A.P., Fonseca I. (2016). High efficacy on diclofenac removal by activated carbon produced from potato peel waste. *Int. J. Environ. Sci. Technol.* 13, 1989–2000. https://doi.org/10.1007/s13762-016-1030-3

Bouchelta C., Medjram M.S., Bertrand O., Bellat J.-P. (2008). Preparation and characterization of activated carbon from date stones by physical activation with steam. *J. Anal. Appl. Pyrolysis* 82, 70–77. https://doi.org/10.1016/j.jaap.2007.12.009

Bouhcain B., Carrillo-Peña D., El Mansouri F., Ez Zoubi Y., Mateos R., Morán A., Quiroga J.M., Zerrouk M.H. (2022). Removal of Emerging Contaminants as Diclofenac and Caffeine Using Activated Carbon Obtained from Argan Fruit Shells. *Appl. Sci.* 12, 2922. https://doi.org/10.3390/app12062922

Bouhcain B., Mansouri F.E., Brigui J., Ruiz S.G., Alonso J.M.Q., Dekkaki H.C., Zerrouk M.H. (2021). Study of elimination of emerging contaminants by adsorption using activated carbon of coconut (amoxicillin - penicillin - theobromine). *AIP Conf. Proc*. 2417, 020001. https://doi.org/10.1063/5.0072592

Boujibar O., Souikny A., Ghamouss F., Achak O., Dahbi M., Chafik T. (2018). CO2 capture using N-containing nanoporous activated carbon obtained from argan fruit shells. *J. Environ. Chem. Eng.* 6, 1995–2002. https://doi.org/10.1016/j.jece.2018.03.005

Cheng N., Wang, B., Wu, P., Lee, X., Xing, Y., Chen, M., Gao, B. (2021). Adsorption of emerging contaminants from water and wastewater by modified biochar: A review. *Environ. Pollut.* 273, 116448. https://doi.org/10.1016/j.envpol.2021.116448

Chuang C.L., Fan M., Xu M., Brown R.C., Sung S., Saha B., Huang C.P. (2005). Adsorption of arsenic(V) by activated carbon prepared from oat hulls. *Chemosphere* 61, 478–483. doi.org/10.1016/j.chemosphere.2005.03.012

Danish M., Birnbach, J., Mohamad Ibrahim, M.N., Hashim, R., Majeed, S., Tay, G.S., Sapawe, N. (2021a). Optimization study of caffeine adsorption onto large surface area wood activated carbon through central composite design approach. *Environ. Nanotechnol. Monit. Manag.* 16, 100594. https://doi.org/10.1016/j.enmm.2021.100594

Danish M., Birnbach J., Mohamad Ibrahim M.N., Hashim R., Majeed S., Tay G.S., Sapawe N. (2021b). Optimization study of caffeine adsorption onto large surface area wood activated carbon through central composite design approach. *Environ. Nanotechnol. Monit. Manag.* 16, 100594. https://doi.org/10.1016/j.enmm.2021.100594

Deblonde T., Cossu-Leguille, C., Hartemann, P. (2011). Emerging pollutants in wastewater: A review of the literature. *Int. J. Hyg. Environ. Health*, The second European PhD students workshop: Water and health ? *Cannes* 2010 214, 442–448. https://doi.org/10.1016/j.ijheh.2011.08.002

Delgado-Moreno L., Bazhari, S., Gasco, G., Méndez, A., El Azzouzi, M., Romero, E., (2021). New insights into the efficient removal of emerging contaminants by biochars and hydrochars derived from olive oil wastes. *Sci. Total Environ.* 752, 141838. https://doi.org/10.1016/j.scitotenv.2020.141838

El-Nabarawy Th., Petro, N.Sh., Abdel-Aziz, S. (1997). Adsorption Characteristics of Coal-based Activated Carbons. II. Adsorption of Water Vapour, Pyridine and Benzene. *Adsorpt. Sci. Technol.* 15, 47–57. https://doi.org/10.1177/026361749701500105

Figueiredo J.L., Pereira, M.F.R., Freitas, M.M.A., Órfão, J.J.M. (1999). Modification of the surface chemistry of activated carbons. *Carbon* 37, 1379–1389. https://doi.org/10.1016/S0008-6223(98)00333-9

Foo K.Y., Hameed, B.H., (2010). An overview of dye removal via activated carbon adsorption process. *Desalination Water Treat.* 19, 255–274. https://doi.org/10.5004/dwt.2010.1214

Gil A., Santamaría, L., Korili, S.A. (2018). Removal of Caffeine and Diclofenac from Aqueous Solution by Adsorption on Multiwalled Carbon Nanotubes. *Colloid Interface Sci.* Commun. 22, 25–28. https://doi.org/10.1016/j.colcom.2017.11.007

GracePavithra K., Jaikumar V., Kumar, P.S., SundarRajan P. (2019). A review on cleaner strategies for chromium industrial wastewater: Present research and future perspective. *J. Clean. Prod.* 228, 580–593. https://doi.org/10.1016/j.jclepro.2019.04.117

Grassi M., Kaykioglu G., Belgiorno, V., Lofrano, G. (2012). Removal of Emerging Contaminants from Water and Wastewater by Adsorption Process, in: Lofrano, G. (Ed.), Emerging Compounds Removal from Wastewater: Natural and Solar Based Treatments, *SpringerBriefs in Molecular Science. Springer* Netherlands, Dordrecht, pp. 15–37. https://doi.org/10.1007/978-94-007-3916-1_2

Gupta V.K., Suhas (2009). Application of low-cost adsorbents for dye removal – A review. *J. Environ. Manage.* 90, 2313–2342. https://doi.org/10.1016/j.jenvman.2008.11.017

Igwegbe C.A., Mohmmadi, L., Ahmadi, S., Rahdar, A., Khadkhodaiy, D., Dehghani, R., Rahdar, S. (2019). Modeling of adsorption of Methylene Blue dye on Ho-CaWO4 nanoparticles using Response Surface Methodology (RSM) and Artificial Neural Network (ANN) techniques. *MethodsX* 6, 1779–1797. https://doi.org/10.1016/j.mex.2019.07.016

Ji Y., Li T., Zhu, L., Wang, X., Lin, Q., (2007). Preparation of activated carbons by microwave heating KOH activation. Appl. Surf. Sci. 254, 506–512. https://doi.org/10.1016/j.apsusc.2007.06.034

Jodeh S., Basalat N., Abu Obaid A., Bouknana D., Hammouti B., Hadda T. B., Jodeh W., Warad I. (2014). Adsorption of some organic phenolic compounds using activated carbon from cypress products, *J. Chem. Pharmac. Res.,* 6 N°2, 713-723

Kankou M. S.'A., N'diaye A. D., Hammouti B., Kaya S. and Fekhaoui M. (2021) Ultrasound-assisted adsorption of Methyl Parathion using commercial Granular Activated Carbon from aqueous solution, *Mor. J. Chem.* 9(4), 832-842

Karimi-Maleh H., Ayati, A., Davoodi R., Tanhaei B., Karimi F., Malekmohammadi S., Orooji Y., Fu, L., Sillanpää M. (2021a). Recent advances in using of chitosan-based adsorbents for removal of pharmaceutical contaminants: A review. *J. Clean. Prod.* 291, 125880. doi.org/10.1016/j.jclepro.2021.125880

Karimi-Maleh H., Ayati, A., Ghanbari, S., Orooji, Y., Tanhaei, B., Karimi, F., Alizadeh, M., Rouhi, J., Fu, L., Sillanpää, M. (2021b). Recent advances in removal techniques of Cr(VI) toxic ion from aqueous solution: A comprehensive review. *J. Mol. Liq.* 329, 115062. doi.org/10.1016/j.molliq.2020.115062

Karimi-Maleh H., Karimi, F., Malekmohammadi, S., Zakariae, N., Esmaeili, R., Rostamnia, S., Yola, M.L., Atar, N., Movaghgharnezhad, S., Rajendran, S., Razmjou, A., Orooji, Y., Agarwal, S., Gupta, V.K., (2020a). An amplified voltammetric sensor based on platinum nanoparticle/polyoxometalate/two-dimensional hexagonal boron nitride nanosheets composite and ionic liquid for determination of N-hydroxysuccinimide in water samples. *J. Mol. Liq.* 310, 113185. doi.org/10.1016/j.molliq.2020.113185

Karimi-Maleh H., Kumar, B.G., Rajendran, S., Qin, J., Vadivel, S., Durgalakshmi, D., Gracia, F., Soto-Moscoso, M., Orooji, Y., Karimi, F., (2020b). Tuning of metal oxides photocatalytic performance using Ag nanoparticles integration. *J. Mol. Liq.* 314, 113588. https://doi.org/10.1016/j.molliq.2020.113588

Karimi-Maleh H., Ranjbari, S., Tanhaei, B., Ayati, A., Orooji, Y., Alizadeh, M., Karimi, F., Salmanpour, S., Rouhi, J., Sillanpää, M., Sen, F., (2021c). Novel 1-butyl-3-methylimidazolium bromide impregnated chitosan hydrogel beads nanostructure as an efficient nanobio-adsorbent for cationic dye removal: Kinetic study. *Environ. Res.* 195, 110809. https://doi.org/10.1016/j.envres.2021.110809

Karimi-Maleh H., Shafieizadeh M., Taher M.A., Opoku F., Kiarii E.M., Govender P.P., Ranjbari S., Rezapour M., Orooji Y. (2020c). The role of magnetite/graphene oxide nano-composite as a high-efficiency adsorbent for removal of phenazopyridine residues from water samples, an experimental/theoretical investigation. *J. Mol. Liq.* 298, 112040. https://doi.org/10.1016/j.molliq.2019.112040

Li E., Liao L., Lv, G., Li, Z., Yang, C., Lu, Y., (2018). The Interactions Between Three Typical PPCPs and LDH. *Front. Chem.* 6.

Luján-Facundo M.J., Iborra-Clar, M.I., Mendoza-Roca, J.A., Alcaina-Miranda, M.I., (2019). Pharmaceutical compounds removal by adsorption with commercial and reused carbon coming from a drinking water treatment plant. *J. Clean. Prod.* 238, 117866. https://doi.org/10.1016/j.jclepro.2019.117866

Melo L.L.A., Ide, A.H., Duarte, J.L.S., Zanta, C.L.P.S., Oliveira, L.M.T.M., Pimentel, W.R.O., Meili, L., (2020). Caffeine removal using Elaeis guineensis activated carbon: adsorption and RSM studies. *Environ. Sci. Pollut. Res.* 27, 27048–27060. https://doi.org/10.1007/s11356-020-09053-z

Memmert U., Peither, A., Burri, R., Weber, K., Schmidt, T., Sumpter, J.P., Hartmann, A., (2013). Diclofenac: New data on chronic toxicity and bioconcentration in fish. *Environ. Toxicol. Chem.* 32, 442–452. https://doi.org/10.1002/etc.2085

Nam S.-W., Choi D.-J., Kim S.-K., Her N., Zoh K.-D. (2014). Adsorption characteristics of selected hydrophilic and hydrophobic micropollutants in water using activated carbon. *J. Hazard. Mater.* 270, 144–152. https://doi.org/10.1016/j.jhazmat.2014.01.037

Nayak A.K., Pal, A., (2020). Statistical modeling and performance evaluation of biosorptive removal of Nile blue A by lignocellulosic agricultural waste under the application of high-strength dye concentrations. *J. Environ. Chem. Eng.* 8, 103677. https://doi.org/10.1016/j.jece.2020.103677

Neeraj G., Krishnan S., Senthil Kumar P., Shriaishvarya K.R., Vinoth Kumar V. (2016). Performance study on sequestration of copper ions from contaminated water using newly synthesized high effective chitosan coated magnetic nanoparticles. *J. Mol. Liq.* 214, 335–346. doi.org/10.1016/j.molliq.2015.11.051

Netzer A., Hughes, D.E., (1984). Adsorption of copper, lead and cobalt by activated carbon. *Water Res.* 18, 927–933. https://doi.org/10.1016/0043-1354(84)90241-0

Padmavathy K.S., Madhu, G., Haseena, P.V., (2016). A study on Effects of pH, Adsorbent Dosage, Time, Initial Concentration and Adsorption Isotherm Study for the Removal of Hexavalent Chromium (Cr (VI)) from Wastewater by Magnetite Nanoparticles. Procedia Technol., *International Conference on Emerging Trends in Engineering, Science and Technology (ICETEST* - 2015) 24, 585–594. https://doi.org/10.1016/j.protcy.2016.05.127

Senthi Kumar P., Kirthika K. (2009). Equilibrium and Kinetic Study of Adsorption of Nickel from Aqueous Solution onto Bael Tree Leaf Powder. *J. Eng. Sci. Technol.* 4.

Portinho, R., Zanella, O., Féris, L.A., (2017). Grape stalk application for caffeine removal through adsorption. *J. Environ. Manage.* 202, 178–187. https://doi.org/10.1016/j.jenvman.2017.07.033

Rathi B.S., Kumar P.S. (2021) Application of adsorption process for effective removal of emerging contaminants from water and wastewater. *Environ. Pollut.* 280, 116995. doi.org/10.1016/j.envpol.2021.116995

Rout, P.R., Zhang, T.C., Bhunia, P., Surampalli, R.Y., (2021). Treatment technologies for emerging contaminants in wastewater treatment plants: A review. *Sci. Total Environ.* 753, 141990. https://doi.org/10.1016/j.scitotenv.2020.141990

S., S., P., S.K., (2018). Influence of ultrasonic waves on preparation of active carbon from coffee waste for the reclamation of effluents containing Cr(VI) ions. *J. Ind. Eng. Chem.* 60, 418–430. https://doi.org/10.1016/j.jiec.2017.11.029

Saravanan A., Jeevanantham, S., Senthil Kumar, P., Varjani, S., Yaashikaa, P.R., Karishma, S., (2020). Enhanced Zn(II) ion adsorption on surface modified mixed biomass – Borassus flabellifer and Aspergillus tamarii: Equilibrium, kinetics and thermodynamics study. *Ind. Crops Prod*. 153, 112613. https://doi.org/10.1016/j.indcrop.2020.112613

Saravanan A., Kumar, P.S., Renita, A.A., (2018). Hybrid synthesis of novel material through acid modification followed ultrasonication to improve adsorption capacity for zinc removal. *J. Clean. Prod.* 172, 92–105. https://doi.org/10.1016/j.jclepro.2017.10.109

Sauvé S., Aboulfadl, K., Dorner, S., Payment, P., Deschamps, G., Prévost, M., (2012). Fecal coliforms, caffeine and carbamazepine in stormwater collection systems in a large urban area. *Chemosphere* 86, 118–123. https://doi.org/10.1016/j.chemosphere.2011.09.033

Senthamarai C., Kumar, P.S., Priyadharshini, M., Vijayalakshmi, P., Kumar, V.V., Baskaralingam, P., Thiruvengadaravi, K. V., Sivanesan, S., (2013). Adsorption behavior of methylene blue dye onto surface modified Strychnos potatorum seeds. *Environ. Prog. Sustain. Energy* 32, 624–632. doi.org/10.1002/ep.11673

Senthil Kumar P., Fernando, P.S.A., Ahmed, R.T., Srinath, R., Priyadharshini, M., Vignesh, A.M., Thanjiappan, A., (2014a). Effect of Temperature on the Adsorption of Methylene Blue Dye Onto Sulfuric Acid–Treated Orange Peel. *Chem. Eng.* Commun. 201, 1526–1547. doi.org/10.1080/00986445.2013.819352

Senthil Kumar P., Fernando, P.S.A., Ahmed, R.T., Srinath, R., Priyadharshini, M., Vignesh, A.M., Thanjiappan, A., (2014b). Effect of Temperature on the Adsorption of Methylene Blue Dye Onto Sulfuric Acid–Treated Orange Peel. *Chem. Eng.* Commun. 201, 1526–1547. doi.org/10.1080/00986445.2013.819352

Senthil Kumar P., Ramalingam S., Senthamarai C., Niranjanaa M., Vijayalakshmi P., Sivanesan S. (2010). Adsorption of dye from aqueous solution by cashew nut shell: Studies on equilibrium isotherm, kinetics and thermodynamics of interactions. *Desalination* 261, 52–60. doi.org/10.1016/j.desal.2010.05.032

Senthil Kumar P., Sivaranjanee R., Vinothini U., Raghavi M., Rajasekar K., Ramakrishnan K. (2014c). Adsorption of dye onto raw and surface modified tamarind seeds: isotherms, process design, kinetics and mechanism. *Desalination Water Treat.* 52, 2620–2633. doi.org/10.1080/19443994.2013.792016

Tangjuank S., Insuk, N., Tontrakoon, J., Udeye, V., (2009). Adsorption of Lead(II) and Cadmium(II) Ions from Aqueous Solutions by Adsorption on Activated Carbon Prepared from Cashew Nut Shells. *Int. J. Chem. Mol. Eng.* 3, 221–227.

Tharaneedhar V., Senthil Kumar P., Saravanan A., Ravikumar C., Jaikumar, V. (2017). Prediction and interpretation of adsorption parameters for the sequestration of methylene blue dye from aqueous solution using microwave assisted corncob activated carbon. *Sustain. Mater. Technol.* 11, 1–11. https://doi.org/10.1016/j.susmat.2016.11.001

Thekkudan V.N., Vaidyanathan, V.K., Ponnusamy, S.K., Charles, C., Sundar, S., Vishnu, D., Anbalagan, S., Vaithyanathan, V.K., Subramanian, S. (2017). Review on nanoadsorbents: a solution for heavy metal removal from wastewater. *IET Nanobiotechnol.* 11, 213–224. https://doi.org/10.1049/iet-nbt.2015.0114

Thommes M., Kaneko K., Neimark A.V., Olivier J.P., Rodriguez-Reinoso F., Rouquerol J., Sing K.S.W. (2015). Physisorption of gases, with special reference to the evaluation of surface area and pore size distribution (IUPAC Technical Report). *Pure Appl. Chem.* 87, 1051–1069. https://doi.org/10.1515/pac-2014-1117

Torrellas S.Á., García Lovera R., Escalona N., Sepúlveda C., Sotelo, J.L., García, J. (2015). Chemical-activated carbons from peach stones for the adsorption of emerging contaminants in aqueous solutions. *Chem. Eng.* J. 279, 788–798. https://doi.org/10.1016/j.cej.2015.05.104

Vaghetti, J.C.P., Lima, E.C., Royer, B., Cardoso, N.F., Martins, B., Calvete, T., (2009). Pecan Nutshell as Biosorbent to Remove Toxic Metals from Aqueous Solution. *Sep. Sci. Technol.* 44, 615–644. https://doi.org/10.1080/01496390802634331

Verlicchi, P., Galletti, A., Petrovic, M., Barceló, D., Al Aukidy, M., Zambello, E., (2013). Removal of selected pharmaceuticals from domestic wastewater in an activated sludge system followed by a horizontal subsurface flow bed — Analysis of their respective contributions. *Sci. Total Environ.* 454–455, 411–425. https://doi.org/10.1016/j.scitotenv.2013.03.044

Westerhoff P., Yoon, Y., Snyder, S., Wert, E., (2005). Fate of Endocrine-Disruptor, Pharmaceutical, and Personal Care Product Chemicals during Simulated Drinking Water Treatment Processes. *Environ. Sci. Technol.* 39, 6649–6663. https://doi.org/10.1021/es0484799

Yaashikaa P.R., Senthil Kumar, P., Varjani, S.J., Saravanan, A., (2019). Advances in production and application of biochar from lignocellulosic feedstocks for remediation of environmental pollutants. *Bioresour. Technol.* 292, 122030. https://doi.org/10.1016/j.biortech.2019.122030

Zbair M., Ainassaari K., Drif, A., Ojala, S., Bottlinger, M., Pirilä, M., Keiski, R.L., Bensitel, M., Brahmi, R., (2018). Toward new benchmark adsorbents: preparation and characterization of activated carbon from argan nut shell for bisphenol A removal. *Environ. Sci. Pollut. Res.* 25, 1869–1882. https://doi.org/10.1007/s11356-017-0634-6